# Waters™

#### Applikationsbericht

# Capsid Protein Analysis of Viral Vector-Based Gene Therapeutics by Hydrophilic Interaction Chromatography

Lindsey D. Ulmer, Kai Rubach, Abraham S. Finny, Balasubrahmanyam Addepalli, Matthew A. Lauber

Waters Corporation, United States

Published on July 25, 2025

#### Abstract

Adeno-associated viruses (AAVs) are difficult to characterize due to their large mass, unequal abundances of viral capsid proteins (VP1, VP2 and VP3), and sequence similarity. In this application note, the utility of the GTxResolve<sup>TM</sup> Premier BEH<sup>TM</sup> Amide 300 Å 1.7 µm Columns is shown for intact capsid protein analysis of AAV viral vectors of different serotypes and with post-translational modifications through the use of hydrophilic interaction liquid chromatography (HILIC). It shows that the use of GTxResolve Premier BEH Amide 300 Å 1.7 µm Columns can help capture the capsid protein details of AAV capsids through HILIC analysis. These studies reveal batch-to-batch and serotype-to-serotype specific variations in potential post-translational modifications (PTMs) and capsid protein composition. These results position HILIC as highly suitable for assessing batch-to-batch specific variations in capsid protein profiles and their PTMs during release testing studies or product development.

#### Introduction

AAVs serve as a carrier of genetic medicine to facilitate the treatment of genetic disorders through gene therapy. Seven recombinant AAVs (engineered for their specificity) have received regulatory approval as of 2024.<sup>1</sup> The AAV capsids comprise of 60 copies of the capsid viral proteins (VPs) VP1, VP2, and VP3. They assemble at a ratio of 1:1:10, respectively. In addition, the VPs have high sequence similarity, with the sequence of VP3 being contained within the sequence of VP2 and the sequence of VP2 being contained within VP1.<sup>2</sup> The large mass of the 60-unit complex and sequence overlap between the VPs makes AAVs difficult to characterize.<sup>3</sup> Antibody-based methods such as enzyme-linked immunosorbent assay (ELISA) or western blot have typically been used to characterize AAVs but are limited by the availability of specific antibodies.<sup>4</sup> HILIC provides an interesting alternative method to characterize AAVs and has been shown to outperform reversed-phase liquid chromatography in some conditions.<sup>5</sup>

The HILIC columns contain stationary phase with polar functional groups such as silica, diol, or amide. The mobile phase contains a high concentration of organic solvent, aprotic solvent-acetonitrile, and a small amount of water. Under these conditions, the analytes partition into a water-rich layer formed on the stationary phase due to high organic content of the mobile phase. Compounds with higher polarity exhibit stronger affinity for the water layer while the less polar compounds elute more quickly. Thus, HILIC allows retention and efficient separation of polar compounds, which are otherwise poorly retained on reversed-phase chromatography columns. A number of biopharmaceuticals including monoclonal antibodies and AAVs are highly polar and therefore suitable for HILIC analysis.

Here, a GTxResolve Premier BEH Amide 300 Å 1.7 μm, 2.1 x 150 mm Column is used for viral capsid protein analysis following chemical-based (guanidine) capsid dissociation. The stationary phase is double batch tested with nucleic acid and protein reference material to ensure performance out of the box for complex analytes such as AAVs. This application note also demonstrates the successful use of bracketed injection or performance optimizing injection sequence (POISe)<sup>6</sup> for improved analyte focusing. This amide-bonded stationary phase coupled with MaxPeak<sup>™</sup> High Performance Surfaces (HPS) Column hardware is compatible with chemical-based (guanidine) dissociation to quickly screen the overall profile of intact proteins in a viral capsid and identify drug substance batch-to-batch variability.

# Experimental

# Sample Preparation

Acetone Precipitation: AAV2 (empty, titer:  $2 \times 10^{13}$  vp/mL, p/n: 449B000, lots: 20-481 and 24-409) and AAV8 (empty, titer:  $2 \times 10^{13}$  vp/mL, p/n: 288B000, lots: 24-227 and 24-337) were purchased from Virovek (Houston TX) and used in these studies. In some cases, 30 μL volume of AAV was treated with 120 μL of cold acetone (-20 °C) and incubated overnight at -20 °C. The samples were centrifuged at 13,000 xg for 10 minutes. Then the supernatant was removed, and the pellet washed with 250 μL 75% acetone and 25% 18.2 MΩ\*cm water at -20 °C. The sample was centrifuged again at 13,000 xg for 10 minutes. The supernatant was removed, and samples were left in the hood to dry for 30 minutes. Once dried, samples were resuspended in 15 μL 6M guanidine (aqueous, Waters<sup>™</sup> p/n: 186010601-3, lot: W6042412) and analyzed on a GTxResolve Premier BEH Amide 300 Å 1.7 μm, 2.1 x 150 mm Column (p/n: 186011251 <

https://www.waters.com/nextgen/global/shop/columns/186011251-gtxresolve-premier-beh-amide-column-300-a-17--m-21-x-150-mm-1-pk.html> ) as described below.

Guanidine Bracketed Injections: 6M guanidine HCl was prepared in 50/50 18.2 M $\Omega$ \*cm water/ACN mixture using solid guanidine hydrochloride from Sigma (p/n: G4505-100G-HC, lot:SLCF2288) and used to inject AAV2 and AAV8 into the column.

#### LC Conditions

| LC system:    | ACQUITY™ Premier UPLC™ System  |
|---------------|--|
| Detection:    | FLR with excitation at 280 nm and emission at 348 nm; UV at 280 nm with a TUV Detector   |
| Column name:  | GTxResolve Premier BEH Amide 300 Å 1.7 µm, 2.1 x<br>150 mm Column  |
| Sample vials: | QuanRecovery <sup>™</sup> MaxPeak Vials (p/n: 186009186)<br>and Polyethylene Septum less Screw Caps (p/n:<br>186004169) for AAV and Pre-Slit PTFE/Silicone |

Septa Caps for ACN (p/n: 186005827)

Injection sequence 1: 3 µL ACN, 4 µL acetone precipitated AAV, 3 µL

ACN

Injection sequence 2: 3  $\mu$ L ACN, 4  $\mu$ L AAV, 3  $\mu$ L 6M guanidine in 50/50

18.2 M $\Omega$  water/CAN

Column temperature: 60 °C

Sample temperature: 5 °C

Mobile phase A: 0.1% TFA in 18.2  $M\Omega^*$ cm water

Mobile phase B: 0.1% TFA in ACN

#### **Gradient Table**

| Time<br>(min) | Flow<br>(mL/min) | %A   | %В   |
|---------------|------------------|------|------|
| 0.00          | 0.20             | 30.0 | 70.0 |
| 3.00          | 0.20             | 30.0 | 70.0 |
| 18.90         | 0.20             | 36.0 | 64.0 |
| 20.10         | 0.20             | 80.0 | 20.0 |
| 21.90         | 0.20             | 80.0 | 20.0 |
| 22.50         | 0.20             | 30.0 | 70.0 |
| 30.00         | 0.20             | 30.0 | 70.0 |

### Results and Discussion

# HILIC Analysis of Aqueous Biopharmaceuticals

In HILIC conditions, the high organic solvent is the weak eluting solvent, while the water is a strong solvent for eluting the polar compounds that are partitioned into the water-rich layer on the stationary phase. Therefore, a difference in elution strength between the sample diluent (aqueous) and high organic mobile phase results in a mismatch leading to peak distortion and even a severe analyte breakthrough. Although adjustment of sample diluent can minimize the mismatch, high proportion of acetonitrile can be counterproductive due to analyte precipitation or denaturation. Breakthrough effect depends on the injection volume. The term critical injection volume is used to describe the maximum injection volume at which breakthrough does not occur. This depends on column volume and retention factor of solute in sample diluent and is typically 0.1-0.3  $\mu$ L aqueous sample for a 2.1 x 150 mm HILIC column. Introducing organic solvent pre-plug before sample can allow sample injection of 2-5% column volume without breakthrough effect. Such a strategy is followed in this application note for AAV capsid protein analysis under HILIC conditions.

#### Acetone Precipitated Sample Preparation

Figure 1 illustrates the HILIC-LC based separation of VP1, VP2, and VP3 from empty AAV2 capsids that were acetone precipitated and resuspended with 6M guanidine-HCl solution. Acetone precipitation concentrates the samples by a factor of two and adds guanidine without diluting the sample. The increased concentration helps increase the signal (data not shown). The addition of guanidine dissociates the AAV into its VP proteins. The sample exhibited a clear, prominent peak for VP3 at about 10.5 minutes with partially resolved proteoforms corresponding to different PTMs on VP3 at 11.0, 11.3, and 11.6 minutes. There are weaker signals for VP1 at 12.6 minutes and VP2 at 13.5 minutes. The VP1 and VP2 peaks are also followed by partially resolved proteoforms for each protein. The weaker signals for VP1 and VP2 are because of the 10:1:1 ratio for VP3, VP1, and VP2, respectively. The separation of VP1, VP2, and VP3 in Figure 1 aligns closely with a previously reported HILIC analysis of AAV2, <sup>9</sup> albeit with additional PTMs. These additional PTMs correspond to different combinations of oxidation and phosphorylation which have been reported previously. <sup>5</sup> The use of a bracketed injection sequence (injecting ACN, then sample, then ACN to solvent match) reduced band broadening and increased peak height, making it more feasible to resolve and detect low intensity proteoforms, such as the differing PTMs on VP1 and VP2 proteins (data not shown). In the absence of sample concentration or bracketed injections, the signal is weak and peaks are broad (data not shown).

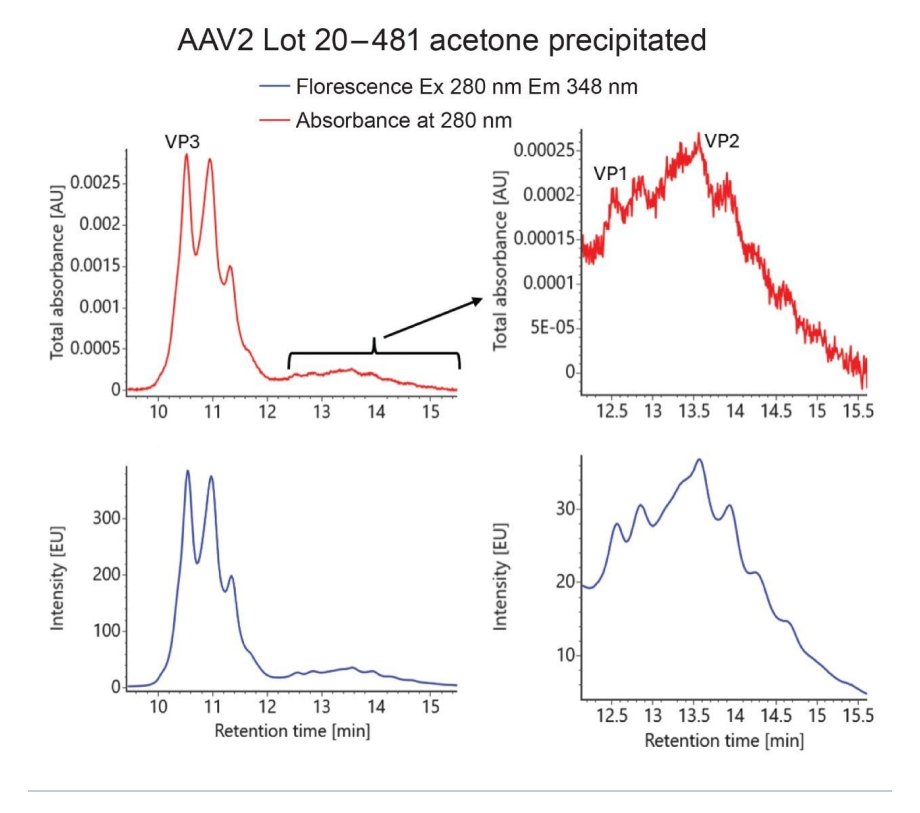


Figure 1. HILIC separation of acetone-precipitated empty AAV2 capsid from a lot 20-481. The absorbance trace at 280 nm is shown in red at the top of the stack, and the fluoroscence profile is shown at the bottom in blue. The chromatogram is annotated to indicate the elution profiles of VP3, VP2, and VP1. Peaks appearing between these labels correspond to PTMs associated with the preceding VP protein. For example, the peak at 11 minutes corresponds to a PTM on VP3. The right side of the figure depicts the zoomed view of the trace to show the VP1 and VP2 profile. Data shown here is not normalized.

Similar to Figure 1, Figure 2 illustrates the separation of VP1, VP2, and VP3 from empty AAV8 capsids that were acetone precipitated and dissolved with 6M guanidine-HCl solution. Similar to AAV2 (Figure 1), there are peaks for VP3 (9.3 minutes), VP2 (13.2 minutes), and VP1 (12.1 minutes) followed by partially resolved PTMs for each VP protein. The observation that AAV8 proteoforms separate in a manner similar to AAV2 demonstrates that the GTxResolve Premier BEH Amide 300 Å (1.7  $\mu$ m, 2.1  $\times$  150 mm) Column is effective in resolving post-translational

modifications on VP proteins across different serotypes.

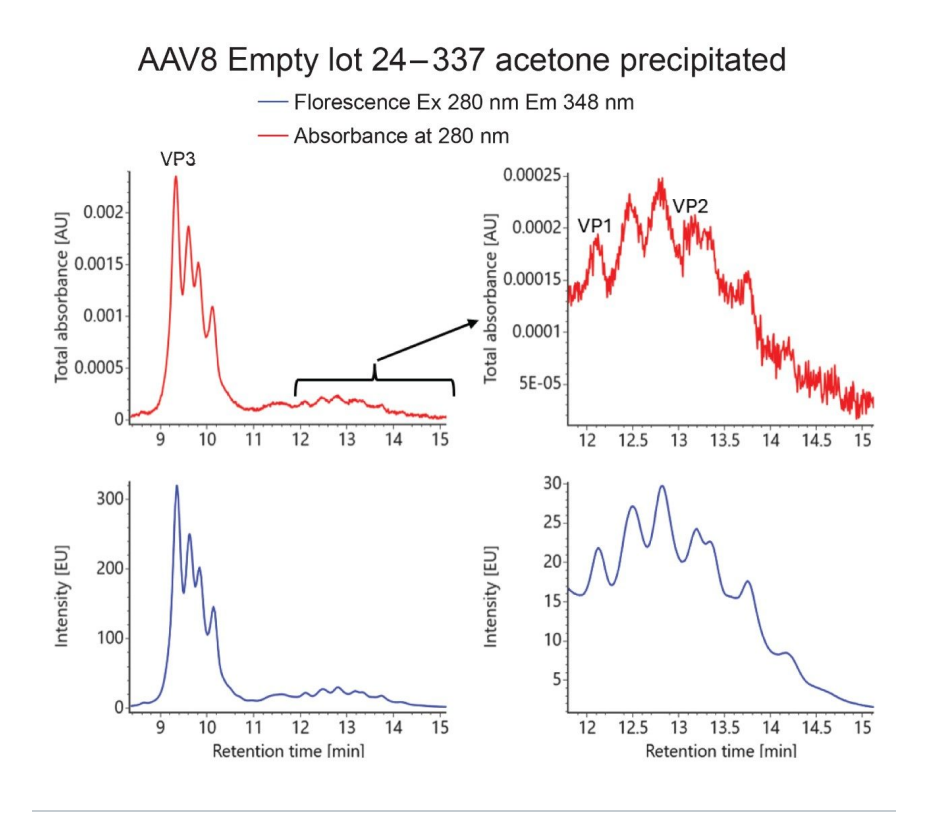


Figure 2. HILIC separation of acetone-precipitated empty AAV8 capsid from a lot 24-337. The absorbance trace at 280 nm is shown in red at the top of the stack, and the fluoroscence profile is shown at the bottom in blue. The chromatogram is annotated to indicate the elution profiles of VP3, VP2, and VP1. Peaks appearing between these labels correspond to post-translational modifications associated with the preceding VP protein. For example, the peak at 9.6 minutes corresponds to a PTM on VP3. The right side of the figure depicts the zoomed view of the trace to show the VP1 and VP2 profile. Data shown here is not normalized.

# Lot-to-Lot Variation in PTM Profiles in AAV Serotypes

Figure 3 illustrates the separation of VP1, VP2, and VP3 achieved from analyzing two different lots of empty AAV2 that were chemically dissociated using different strategies. Both sample preparation types were chemically

dissociated with guanidine, but the contact with guanidine-hydrochloride was accomplished in two separate ways. Samples were either acetone precipitated and dissolved in 6M guanidine then analyzed with bracketed injections (injecting ACN, acetone precipitated AAV, then ACN) or directly bracketed with 6M guanidine in 50/50 water/ACN (injecting ACN, AAV, then 6M guanidine in 50/50 water/ACN) but without prior acetone precipitation. The top row in Figure 3 shows VP protein profiles for acetone precipitated AAV2, and the bottom row shows VP protein profiles for guanidine-bracketed AAV2. Both sample preparation methods yield similar profiles. The guanidine bracketed method exhibited a slight band broadening that results in lower resolution, although the peaks corresponding to different proteoforms are discernible. However, positioning the guanidine before the AAV (guanidine, then AAV, then ACN) exhibited severe peak broadening and severe loss in resolution (data not shown). Either sample preparation method seems suitable to analyze chemically dissociated AAVs as illustrated by the similar profiles for each method in Figure 3. Although the acetone precipitation method requires more involved sample preparation, the signal intensity was much improved and better than that of direct injection. On the other hand, the guanidine bracketed sample exhibited band broadening.

Figure 3 also illustrates lot-to-lot differences of AAV2. The left half of Figure 3 illustrates results from lot 20-481 (Virovek p/n: 449B000) and the right half of Figure 3 illustrates results from lot 24-409 (Virovek p/n: 449B000). Both lots have VP3, VP2, and VP1 peaks at similar retention times. Lot 20-481 has more peaks for each VP protein, indicating there are more PTMs present in lot 20-481. This illustrates the utility of the GTxResolve Premier BEH Amide 300 Å (1.7  $\mu$ m, 2.1  $\times$  150 mm) Column in visualizing lot-to-lot variation in AAVs, especially for identifying differences in the PTMs.

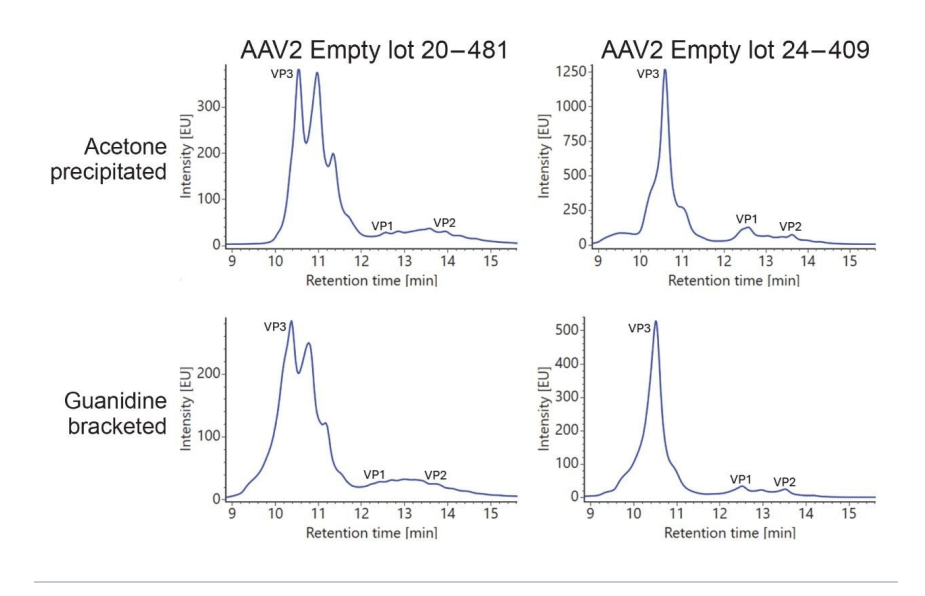


Figure 3. HILIC separation of acetone-precipitated and guanidine-bracketed empty AAV2 capsid from lot 20-481 and lot 24-337. On the left side, fluorescence profiles for lot 20-481 are shown, and on the right side, fluorescence profiles for lot 24-409 are shown. The top row includes the fluorescence profile for acetone-precipitated samples, and the bottom row includes the fluoroscence profiles for guanidine-bracketed samples. The chromatograms are annotated to indicate the elution profiles of VP3, VP2, and VP1. Peaks appearing between these labels correspond to post-translational modifications associated with the preceding VP protein. For example, the peak at 11 minutes corresponds to a PTM on VP3. Data shown here is not normalized.

Table 1 indicates the VP ratios for the different AAV2 lots and sample preparation types when using absorbance peak areas for calculations. The values are close to the expected 1:1:10 for VP1:VP2:VP3 but seem to differ between the lots. The deviations that were observed from 1:1:10 are similar to what has been previously reported. <sup>5, 9</sup> Lot 20-481 has a higher ratio for VP2 (1 instead of 0.83 for acetone-precipitated and 1 instead of 0.55 for guanidine bracketed), while lot 24-409 has a higher ratio for VP1 (1 instead of 0.61 for acetone-precipitated and 1 instead of 0.46 for guanidine bracketed). Given the absorbance-based ratios in Table 1, it can be noted that there are some differences between the sample preparation methods with the acetone precipitated samples yielding higher VP3 ratios (10.5 instead of 7.18 for lot 20-481 and 14.7 instead of 10.56 for lot 24-409). As seen in Table 1,

the guanidine-bracketed samples show lower ratios for the least abundant proteins—VP1 in lot 20-481 and VP2 in lot 24-409. This impact on the lowest abundance proteins suggests that the variation in calculated ratios for different sample preparation methods is likely due to increased band broadening in the guanidine-bracketed approach, which can hamper the detection of low-intensity species.

Table 2 indicates the VP ratios for the different AAV2 lots and sample preparation types when using fluorescence peak areas for calculations. Compared to the absorbance-based values in Table 1, the values calculated from fluorescence are closer to a 1:1:10 ratio, and there is less difference between sample preparation methods. The discrepancies between the ratios calculated from absorbance and fluorescence traces are likely due to the higher signal intensity in fluorescence, which produces smoother, less noisy signals. The higher fluorescence signal intensity observed in Figure 1 suggests that fluorescence is better suited towards quantitative analysis.

| Lot    | Sample prep            | VP1  | VP2  | VP3   |
|--------|------------------------|------|------|-------|
| 20-481 | Acetone precipitated   | 0.61 | 1    | 10.5  |
| 20-481 | Guanidine<br>bracketed | 0.46 | 1    | 7.18  |
| 24-409 | Acetone precipitated   | 1    | 0.83 | 14.7  |
| 24-409 | Guanidine<br>bracketed | 1    | 0.55 | 10.56 |

Table 1. The VP ratios for AAV2 absorbance traces are shown.
Ratios were determined using chromatographic peak areas of absorbance traces, including contributions from any PTMs on VP proteins.

| Lot    | Sample prep            | VP1  | VP2  | VP3   |
|--------|------------------------|------|------|-------|
| 20-481 | Acetone precipitated   | 0.67 | 1    | 9.73  |
| 20-481 | Guanidine<br>bracketed | 0.63 | 1    | 10.14 |
| 24-409 | Acetone precipitated   | 1    | 0.86 | 12.6  |
| 24-409 | Guanidine<br>bracketed | 1    | 0.5  | 11.67 |

Table 2. The VP ratios for AAV2 fluorescence traces are shown. Ratios were determined using chromatographic peak areas of fluorescence traces, including contributions from any PTMs on VP proteins.

Figure 4 illustrates the separation of VP1, VP2, and VP3 from the analysis of two different lots of empty AAV8 following chemical dissociation, similar to Figure 3 for AAV2. The top row in Figure 4 shows VP protein profiles for acetone precipitated AAV8, and the bottom row shows VP protein profiles for guanidine bracketed AAV8. Similar to AAV2 in Figure 3, acetone precipitated samples exhibited improved peak intensity and profiles compared to direct injection. However, both sample preparation methods yielded similar profiles with increased band broadening in the guanidine-bracketed sample. The similarities observed in the application of sample preparation methods across different serotypes in Figures 3 and 4 indicate that either method is suitable for analyzing various serotypes.

Figure 4 also illustrates the lot-to-lot differences of AAV8. The left half of Figure 4 illustrates results from lot 24-227 (Virovek p/n: 288B000) and the right half of Figure 4 illustrates results from lot 24-337 (Virovek p/n: 288B000). Both lots produce the VP3, VP2, and VP1 peak at similar retention times. Lot 24-337 has more peaks for each VP protein, indicating there are more PTMs present in lot 24-337.

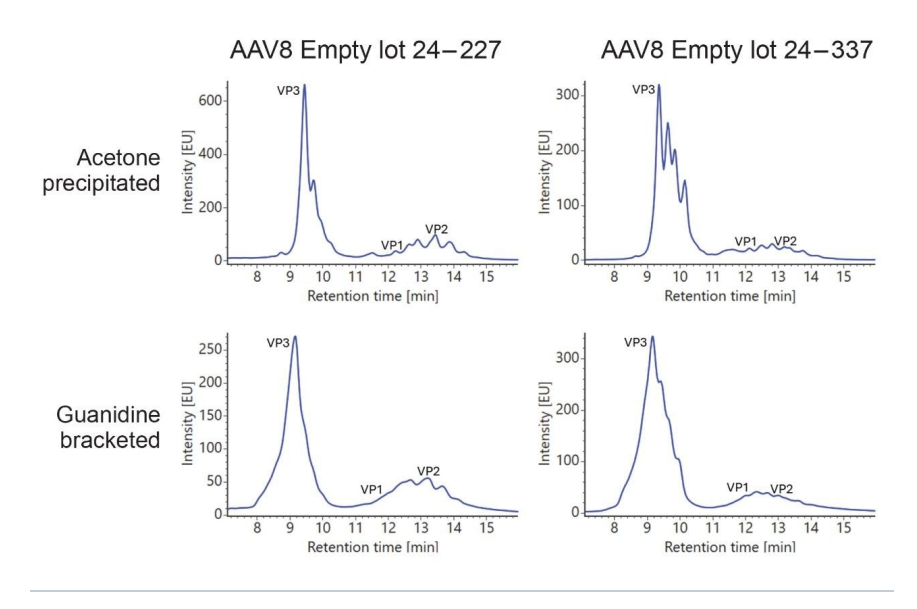


Figure 4. HILIC separation of acetone-precipitated and guanidine-bracketed empty AAV8 capsid from lot 24-227 and lot 24-337. On the left side, fluorescence profiles for lot 24-227 are shown, and on the right side, fluorescence profiles for lot 24-337 are shown. The top row includes the fluorescence profile for acetone-precipitated samples, and the bottom row includes the fluoroscence profiles for guanidine-bracketed samples. The chromatograms are annotated to indicate the elution profiles of VP3, VP2, and VP1. Peaks appearing between these labels correspond to PTMs associated with the preceding VP protein. For example, the peak at 9.6 minutes corresponds to a PTM on VP3. Data shown here is not normalized.

Table 3 provides the VP ratios for the different AAV8 lots and sample preparation types when using absorbance peak areas for calculations. The values are close to the expected 1:1:10 for VP1:VP2:VP3 but differ some between the lots. The deviations that were observed from 1:1:10 are similar to what has been previously reported.<sup>5, 9</sup> Both lots 24-227 and 24-337 have higher ratios for VP2 than VP1, and lot 24-227 has higher values for VP2 than lot 24-337 does with values over two instead of values over 1. Given the absorbance-based ratios in the Table 3, it can be concluded that there are some differences between the sample preparation methods for lot 24-227, but lot 24-337 is quite similar with both sample preparation methods. Lot 24-227 has a higher VP3 ratio (10.59) for the acetone-precipitated sample than for the guanidine bracketed sample (6.07). This is a different effect than Table

1 exhibits for AAV2 where both lots had lower ratios for the least abundant protein with guanidine-bracketed samples. The AAV8 samples are also more similar between the two lots than the AAV2 lots were in that AAV8 lots analyzed had the lowest ratio for VP1.

Table 4 outlines the VP ratios for the different AAV8 lots and sample preparation types when using fluorescence peak areas for calculations, providing similar results to the absorbance-based values in Table 3. Lot 24-227 has a lower VP3 ratio for the guanidine-bracketed sample preparation method when using either absorbance or fluorescence. The increased band broadening from the guanidine-bracketed method is resulting in a lower VP3 ratio. This differs from the results for AAV2 because the differences between sample preparation methods were lessened when using fluorescence values for AAV2 in Table 2. This suggests that different serotypes may be best analyzed using different detection or sample preparation methods. In this case, fluorescence is better suited for quantitative analysis due to the increased peak intensity observed in Figure 2.

| Lot    | Sample prep            | VP1 | VP2  | VP3   |
|--------|------------------------|-----|------|-------|
| 24-227 | Acetone precipitated   | 1   | 2.89 | 10.59 |
| 24-227 | Guanidine<br>bracketed | 1   | 2.25 | 6.07  |
| 24-337 | Acetone precipitated   | 1   | 1.12 | 11.33 |
| 24-337 | Guanidine<br>bracketed | 1   | 1.10 | 11.20 |

Table 3. The VP ratios for AAV8 absorbance traces are shown. Ratios were determined using chromatographic peak areas of absorbance traces, including contributions from any PTMs on VP proteins.

| Lot    | Sample prep            | VP1 | VP2  | VP3   |
|--------|------------------------|-----|------|-------|
| 24-227 | Acetone precipitated   | 1   | 2.67 | 8.78  |
| 24-227 | Guanidine<br>bracketed | 1   | 1.94 | 5.84  |
| 24-337 | Acetone precipitated   | 1   | 1.21 | 11.85 |
| 24-337 | Guanidine<br>bracketed | 1   | 1.08 | 11.15 |

Table 4. The VP ratios for AAV8 fluorescence traces are shown. Ratios were determined using chromatographic peak areas of fluorescence traces, including contributions from PTMs on VP proteins.

#### Conclusion

Here, the separation of AAV capsid proteins following chemical-based denaturation is demonstrated using either acetone-precipitation followed by resuspension with guanidine HCl or injections bracketed with guanidine. Bracketed injections minimized the breakthrough and improved the peak shape. Acetone precipitation led to improved peak intensity and without any additional artifacts. The obtained AAV2 and AAV8 profiles align closely with previous HILIC analyses.<sup>5</sup> By expanding this analysis to different lots, it was possible to identify lot-to-lot variation by identifying different numbers of PTMs on VP proteins from different lots for AAV2 and AAV8. These observations strongly suggest the need for characterizing viral capsid proteoforms during development and release testing to avoid differences in associated PTM profiles and the host response. Further, these studies also establish the utility of GTxResolve Premier BEH Amide 300 Å 1.7 μm, 2.1 x 150 mm Columns for a quick 30-minute capsid protein analysis of AAV serotypes during development and deployment of drug product.

#### References

- 1. Wang, J.-H.; Gessler, D. J.; Zhan, W.; Gallagher, T. L.; Gao, G. Adeno-associated virus as a delivery vector for gene therapy of human diseases. *Signal Transduct. Target. Ther.* 2024, 9, 78. https://doi.org/10.1038/s41392-024-01780-w < https://doi.org/10.1038/s41392-024-01780-w > .
- 2. Clark, M. F.; Adams, A. N. Characteristics of the Microplate Method of Enzyme-Linked Immunosorbent Assay for the Detection of Plant Viruses. *J. Gen. Virol.* 1979, *45* (1), 209–213. https://doi.org/10.1099/0022-1317-45-1-209 <a href="https://doi.org/10.1099/0022-1317-34-3-475">https://doi.org/10.1099/0022-1317-34-3-475</a>.
- Ryan, J. P.; Kostelic, M. M.; Hsieh, C.-C.; Powers, J.; Aspinwall, C.; Dodds, J. N.; Schiel, J. E.; Marty, M. T.; Baker, E. S. J. Am. Soc. Mass Spectrom. 2023, 34 (12), 2811–2821. https://doi.org/10.1021/jasms.3c00321 < https://doi.org/10.1021/jasms.3c00321> .
- 4. Gimpel, A. L.; Katsikis, G.; Sha, S.; Maloney, A. J.; Hong, M. S.; Nguyen, T. N. T.; Wolfrum, J.; Springs, S. L.; Sinskey, A. J.; Manalis, S. R.; Barone, P. W.; Braatz, R. D. Analytical methods for process and product characterization of recombinant adeno-associated virus-based gene therapies. *Mol. Ther. Methods Clin. Dev.* 2021, 21, 237–251. https://doi.org/10.1016/j.omtm.2021.02.010 <a href="https://doi.org/10.1016/j.omtm.2021.02.010">https://doi.org/10.1016/j.omtm.2021.02.010</a> .
- 5. Liu, A. P.; Patel, S. K.; Xing, T.; Yan, Y.; Wang, S.; Li, N. Characterization of Adeno-Associated Virus Capsid Proteins Using Hydrophilic Interaction Chromatography Coupled with Mass Spectrometry. J. Pharm. Biomed. Anal. 2020, 189, 113481. https://doi.org/10.1016/j.jpba.2020.113481 <a href="https://doi.org/10.1016/j.jpba.2020.113481">https://doi.org/10.1016/j.jpba.2020.113481</a>.
- 6. Fekete, S.; Imiolek, M.; Lauber, M. Advantages of Sequential or Bracketed Injection Methods to Improve the Chromatographic Analysis of Biotherapeutics. LCGC International, 2024, 20, 17–24.
- 7. Chapel, S.; Rouvière, F.; Peppermans, V.; Desmet, G.; Heinisch, S. A Comprehensive Study on the Phenomenon of Total Breakthrough in Liquid Chromatography. *J. Chromatogr. A.* 2021, *1653*, 462399. DOI: 10.1016/j.chroma.2021.462399 <a href="https://doi.org/10.1016/j.chroma.2021.462399">https://doi.org/10.1016/j.chroma.2021.462399</a>.
- 8. Chapel, S.; Rouvière, F.; Heinisch, S. Comparison of Existing Strategies for Keeping Symmetrical Peaks in On-Line Hydrophilic Interaction Liquid Chromatography x Reversed-Phase Liquid Chromatography Despite Solvent Strength Mismatch. *J. Chromatogr. A.* 2021, *1642*, 462001. DOI: 10.1016/j.chroma.2021.462001 < https://www.sciencedirect.com/science/article/abs/pii/S0021967321001254> .
- Beaumal, C.; Guapo, F.; Smith, J.; Carillo, S.; Bones, J. Combination of Hydrophilic Interaction Liquid Chromatography and Top-Down Mass Spectrometry for Characterisation of Adeno-Associated Virus Capsid Proteins. *Anal. Bioanal. Chem.* 2025, 417 (10), 2345–2358. https://doi.org/10.1007/s00216-025-05874-4

https://doi.org/10.1007/s00216-025-05874-4>.

#### **Featured Products**

ACQUITY Premier System <

https://www.waters.com/nextgen/global/products/chromatography/chromatography-systems/acquity-premier-system.html>

ACQUITY UPLC and ACQUITY Premier FLR Detectors <

https://www.waters.com/nextgen/global/products/chromatography/chromatography-detectors/acquity-uplc-and-acquity-premier-flr-detectors.html>

ACQUITY UPLC and ACQUITY Premier Tunable UV Detectors <

https://www.waters.com/nextgen/global/products/chromatography/chromatography-detectors/acquity-uplc-and-acquity-premier-tunable-uv-detectors.html>

720008933, July 2025



© 2025 Waters Corporation. All Rights Reserved.

Nutzungsbedingungen Datenschutzhinweis Marken Karriere Rechtliche Hinweise und Datenschutzhinweise Cookies Cookie-Einstellungen